International Research Journal of Engineering and Technology (IRJET) e-ISSN: 2395-0056
Volume: 06 Issue: 05 | May 2019 www.irjet.net p-ISSN: 2395-0072

Influence of Temperature on Tensile Properties and Fracture Behavior of High Strength Stainless Steel

Koteswara Rao Kondisetti[1], Dheeraj Kondisetti[2]

[1]Assistant Professor, Chaitanya Bharathi Institute of Technology, Gandipet, Hyderabad, Telangana, India
[2]Project Engineer, G Stephens Inc., Akron, Ohio, USA

Abstract - *The history of steel dates back to the 17th century and has been instrumental in the betterment of every aspect of our lives ever since, from the pin that holds the paper together to the reinforcement in the construction industry. Path breaking improvements in manufacturing techniques, access to advanced machinery and understanding of factors like heat treatment, corrosion resistance have aided in the advancement in the properties of steel in the last few years. In this research the results of a study aimed at the influence of temperature on tensile fracture behavior of stainless steel 2304 is discussed. The microstructure of the as received steel was examined and characterized for the nature and morphology of the grains and the presence of other intrinsic features in the microstructure. The tensile tests were done on a fully automated closed-loop servo-hydraulic test machine at room temperature as well as elevated temperature. The failed samples of high strength steels were examined in a scanning electron microscope for understanding the fracture behavior. The factors contributing to failure are briefly discussed in light of the conjoint and mutually interactive influences of intrinsic microstructural effects.*

Key Words: Duplex Stainless Steel, Tensile Strength, Fracture Behaviour, Damage analysis.

1. INTRODUCTION

In the domain encompassing materials, science and engineering, high cycle fatigue has been defined to be the end result of progressive, localized, and permanent structural damage that often occurs when a material and/or structure is subjected to tensile stress and cyclic fatigue [1]. In actual practice, two aspects of the fatigue properties of a material must be considered. These are, (a) fatigue life, and (b) fatigue crack growth behavior. In this research study, preliminary experiments were conducted with the primary objective of understanding the influence of test temperature on tensile behavior of a high strength stainless steel. Test specimens of the chosen stainless steel were deformed at ambient temperature and an elevated temperature. The elevated temperature chosen was 205^0C. The results are analyzed and fractographic observation of the fracture surface was used to provide an understanding of the microscopic mechanisms governing the fracture.

2. LITERATURE REVIEW

2.1 Background

The gathering of metals based entirely on compositions, which includes the family of stainless steels initiated way back in 1913 in the city of Sheffield, England. Harry Brierley was attempting various combinations and as could be expected he noticed that the specimens while being cut during one of these trials failed show evidence of rusting and were also found hard to carve. Upon further exploration of this curious metal he found that it contained around 13% chromium. This was immediately classified as stainless steel. This unique property offered by stainless steel led to its selection and use purposes of cutlery. It was cutlery made from stainless steels that eventually made the company based in Sheffield very popular. At around the same time sustained advances were being made in France in the domain spanning steels, which culminated in the development and emergence of austenitic stainless steels. As of this date, the overall utilization of stainless steel is continuing to grow in industries [2].

2.2 The Family of Steels

Stainless steels are iron-based compounds containing around 10.5% chromium. This does result in a defensive self-mending oxide film, which is the primary motivation behind why this class of steels has been given the trademark "stainlessness". The capacity of the thin oxide layer to mend itself implies that this steel is safe against corrosion regardless of the severity of the surrounding environment and the extent of corrosion on the surface. This is not the situation when carbon steels or low amalgam steels are shielded from consumption using either metallic coatings made of zinc or cadmium, or by the use of natural coatings, such as paint [4]. Although every stainless steel relies upon the use of chromium, other alloying elements are also regularly added with the primary purpose of achieving a better combination of properties. Depending upon the exact chemical composition, the family of stainless steels can be broadly classified to be the following: (i) Austenitic Stainless steels, (ii) Ferritic Stainless Steels, (iii) Martensitic Stainless Steels, (iv) Duplex Stainless steels, and (v) Precipitation hardening stainless steels [3].

2.3 Characteristics of Stainless Steel

The overall characteristics of the family of stainless steels in comparison with the family of carbon steels are essentially the following [4]:
(a) High work hardening rate
(b) Good ductility
(c) High strength and hardness
(d) Improved strength at elevated temperatures
(e) Good corrosion resistance
(f) Improved toughness at cryogenic temperatures
(g) Lower magnetic response (for the family of austenitic stainless steels)
(h) Can retain a corrosion resistant surface in the finished product.

2.4 Stainless Steel as Reinforcement for Civil Construction Industry

Stainless steel is chosen for its corrosion resistance, strength and long life. The increase in cost arising from utilizing stainless steel as strengthening bars in concrete ranges from one to fifteen percent depending upon overall complexity of the structure. At a point when Life Cycle Cost and a longer life for the reinforcing bar, up to 125 years, occurs then stainless steel is a financially effective choice as reinforcing material. Stainless steels offer either the same or even higher strength than carbon steel, depending on the alloy chosen. The chosen stainless steel compositions have natural corrosion resistance and improved resistance to pitting corrosion, crevice corrosion, and even stress corrosion cracking. The group of elements can even be effectively framed into 3-D twists, if required, welded and made accessible in attractive and non-magnetic alloy compositions while offering the attributes of both high and low temperature strength [5].

2.5 Tensile and Fatigue Behavior of Stainless Steel

E.S Puchi-Cabrera and co-workers [6], published their research findings on the fatigue behavior of an AISI 316L stainless steel coated with a PVD titanium nitride (TiN) deposit and concluded that coating a 316L stainless steel with TiN offered a substantial improvement in fatigue properties in comparison with the uncoated substrate. The increase in fatigue life was found to be significantly dependent on the magnitude of alternating stress applied to the material. At a low maximum alternating stress (460 MPa) the observed improvement in fatigue life was as high as 2119%, whereas, at a higher value of the maximum alternating stress (510 MPa) an increase in fatigue life of up to 400% was achieved. The fatigue limit increased by 22%. There was no substantial increase in yield strength of the coated material.

K.K.Ray and co-workers [7], studied the influence of mean stress on fatigue damage of AISI 304 LN stainless steel. They conducted a series of fatigue experiments on 304LN stainless steel, using stress-control mode, for a number of combinations of mean stress and stress amplitude. They observed the extent of strain accumulation in the selected AISI 304LN stainless steel to increase with an increase in magnitude of the peak stress of imposed cyclic loading. The magnitude of strain accumulation was found to be only marginal when the tests were carried out under symmetric loading, but its magnitude was considerable when the tests were done under asymmetric loading, despite the mean stress being positive or negative. When magnitude of the mean stress was kept constant, the number of cycles to cause fatigue failure (Nf) decreased with an increase in amplitude of the alternating stress.

H. Nishi and co-workers [8], studied the fatigue behavior on weldment of austenitic stainless steel for use in the ITER vacuum vessel. Locations of incomplete penetrations (IP) behaved and propagated as a crack. Most of total fatigue life for the weldment was predominantly time spent in crack propagation. The crack propagation rates of the weldment were very much in accordance with those of the weld metal. The fatigue lives were estimated using fracture mechanics principles based on crack propagation rates of the weld metal. The fatigue strength of the weldment was found to be noticeably lower than that of the smooth specimen. The effect of incomplete penetration (IP) on fatigue strength of the weldment is serious problem even if the IP is small.

M.F. Buchely and co-workers [9], studied the effect of shielded metal arc welding (SMAW) manufacturing process on high-cycle fatigue of AISI 304 base metal using AISI 308L filler metal. They concluded the microstructure of the weld deposits to be austenitic stainless steel and retained ferrite to be both in ventricular and lathy morphology. The dendrite arm spacing was found to be smaller for specimens that used a “high” heat input during welding. It was found that a higher ferrite number (FN) was responsible for lower hardness of the weld deposits. The modified Goodman criterion was found to work well for the conditions studied. It was found that at a “low” heat input the deposits offered the highest resistance to high-cycle fatigue.

M. Topic and co-workers [10], published their research findings on the effect of cold work and heat treatment on the fatigue behavior of 3CR12 corrosion resistant steel wire. The mechanical properties of 3CR12 steel wire was found to increase with increased drawing strain. Further, the drawing strain increased the fatigue limit of initially annealed 3CR12 steel wire for both the smooth and notched test samples. An application of the cold drawn 3CR12 steel wire was limited to low stress fatigue conditions. Drawing of quenched 3CR12 steel was significantly improved and much easier to achieve when compared to drawing of 3CR12 steel that had an initial annealed microstructure. Quenching and successive drawing did contribute to improving the fatigue strength. The dual-phase microstructure had a significant benefit in terms of fatigue behavior; it delayed crack initiation and retarded crack propagation. A noticeable change in fatigue fracture mode, from predominantly transgranular to brittle, was a major limiting factor for the application of quenched-drawn 3CR12 steel wires when the cyclic stresses were higher than 15% of the fatigue limit.

Zahida begum and co-workers [11], studied the tensile and corrosion fatigue behavior of austenitic stainless steels. They found Type 304 stainless steel to possess the highest yield strength and ultimate tensile strength, and resultant lower ductility. The other steels ranked in order of decreasing yield strength and tensile strength, and increased ductility were Type 316LN stainless steel, Type 316 stainless steel and Type 316L stainless steel. Fractographic studies revealed corrosion fatigue cracking to be wholly transgranular for all of the steels. For all the steels, transgranular cracking of austenite was evident at mean stress values of 200 MPa and 250 MPa. No visibly distinct striations were observed. At lower values of mean stress (100 MPa and 150 MPa), fine striations were observed in all the stainless steels examined.

Stainless steel is a good corrosion resistant material. Corrosion is one of the major problems in construction Industry. Over twenty six percent of the bridges in the United States are structurally deficient or functionally obsolete. Corrosion of steel used in structures like bridges and buildings is a problem that has gained increased interest and focused concern [13-17].

3. THE MATERIAL CHOSEN

3.1 Material

The material chosen for this study was the Duplex Stainless Steel 2304 supplied by Salit Specialty Rebar. The chemical composition of this steel is provided in Table 3.1. Presence of carbon provides not only solid solution strengthening but also hardenability through the formation and presence of alloy carbides in the microstructure. The presence of elements like chromium [Cr] assists in both the formation and presence of carbide particles, which contributes to enhancing strength of the steel matrix. However, the presence and distribution of carbide particles in the microstructure is detrimental to fracture toughness or impact resistance arising as a consequence of increasing the number of potential sites for initiation of fine microscopic cracks. Presence of nickel [Ni] facilitates in lowering the transition temperature while simultaneously enhancing toughness and stabilizing any austenite that is present in the material [12].

Table -3.1: Nominal chemical composition of Stainless Steel 2304 (Weight Percent)

Material	Fe	Cr	Ni	Mn	Si	Cu	Mo	N	P	C	B	S
2304 Stainless Steel	70.55	22.84	3.64	1.72	0.46	0.31	0.26	0.17	0.02	0.02	.002	.001

3.2 Test Specimen Preparation

Full length rebar's made of duplex stainless steel are often chosen for use potentially viable reinforcements for reinforced concrete structures. The rebar was cut into small pieces, each of size 2.5 inches, as shown in Figure 3.1. The cut samples were sent to a professional machining facility based in Pennsylvania for the purpose of machining in conformance with standards specified in ASTM E-8, as shown in Figure 3.2. The machined test final specimen is shown in Figure 3.3.

Fig -3.1: Rebar cut pieces before machining to desired shape

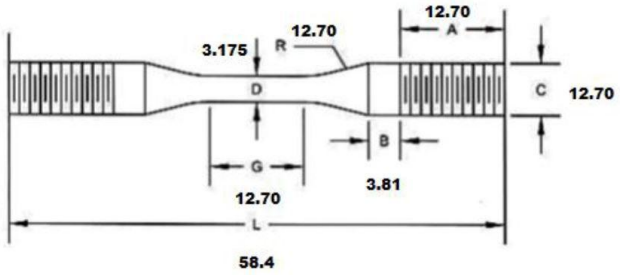

Fig -3.2: A schematic of the cylindrical test specimen used for mechanical testing

Fig -3.3: Typical specimen after machining

4. EXPERIMENTAL PROCEDURES

4.1 Initial Microstructure Characterization

An initial characterization of the micro-structure of the as-provided material was done using a low magnification optical microscope. Samples of required size were cut from the as-received material, which is stainless steel 2304 and mounted in epoxy and polished using a series of silicon carbide impregnated emery paper having different grit size of 240-grit, 320-grit, 400-grit and 600-grit using copious amounts of water both as a lubricant and coolant. Subsequently, the steel sample was mechanically polished using five-micron alumina powder suspended in distilled water. Fine polishing to a perfect mirror-like finish of the surface was achieved using a solution of one-micron alumina powder suspended in distilled water as the lubricant. Subsequent to polishing, the sample was subsequently

etched using a reagent, that is a solution mixture of 16.67 pct. Hydrochloric acid (HCl) and 83.33 pct. distilled water (H2O). In other words, 200 ml of HCl for 1000 ml of H2O. This is termed as Beraha's tint etch. The surface of the steel sample which was polished and etched was then observed in an optical microscope and photographed using standard bright field illumination technique, shown in the Figure 4.1.

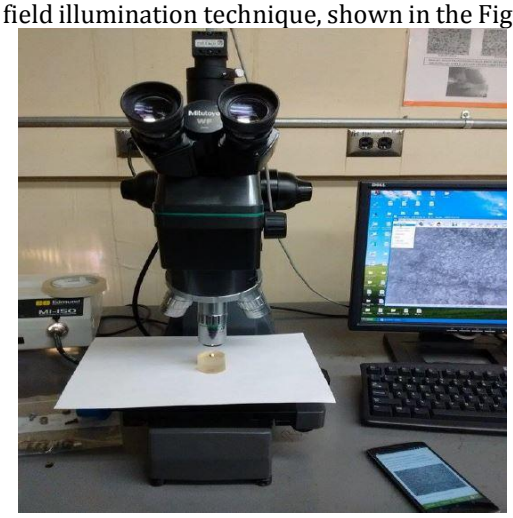

Fig -4.1: Low magnification optical microscope for examining microstructure

4.2 Tensile Tests

Uniaxial tests were conducted on an INSTRON-8500 plus, a closed loop, fully automated servo-hydraulic mechanical test machine, using a 100 KN load cell. The tests were performed both at room temperature and at an elevated temperature in the laboratory air environment [Relative Humidity of 55%]. Test samples of the chosen steel were deformed at a constant strain rate of 0.0001/sec. An axial 12.5mm gage length clip on extensometer was attached to the test sample, utilizing rubber bands for tests at room temperature and steel springs for tests at the elevated temperature, to provide a measure of strain during uniaxial stretching. The stress and strain measurements, parallel to the load line, were recorded on a PC–based data acquisition system (DAS).

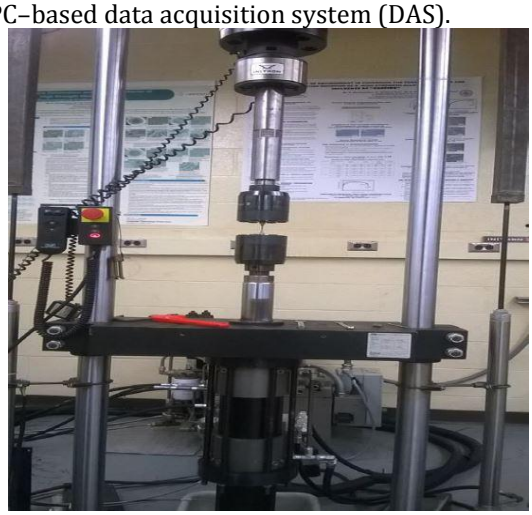

Fig -4.2: Test setup for tensile testing at room temperature

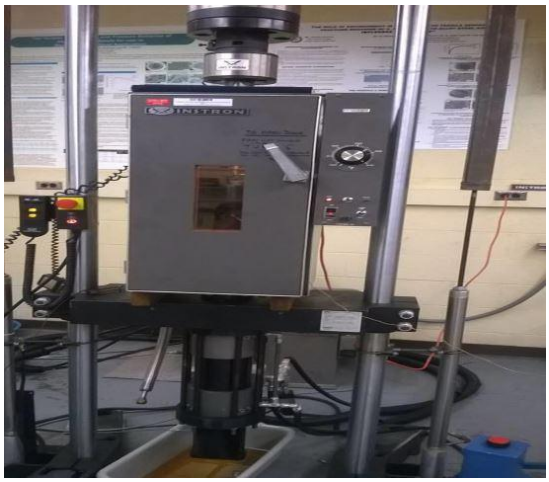

Fig -4.3: Test setup for tensile testing at 205^0C

4.3 Failure Damage Analysis

Fracture surfaces of the deformed and failed tensile specimens were examined in a scanning electron microscope (SEM). This was done to help establish the macroscopic fracture mode while concurrently characterizing the fine-scale features on the fracture surface so as to help establish the microscopic mechanisms governing fracture. The difference between macroscopic and microscopic fracture mechanisms is based entirely on the level of magnification at which the surface was observed and the micrographs taken. The overall nature of failure is referred to as the macroscopic mode while failure processes occurring at the local level are referred to as microscopic mechanisms. These mechanisms include the following: (i) microscopic void formation, (ii) microscopic void growth, and (iii) eventual coalescence to form one or more fine microscopic cracks. The microscopic cracks grow and coalesce to form macroscopic cracks.

5. RESULTS AND DISCUSSIONS

5.1 Initial Microstructure

The microstructure of the material chosen is an important factor to be taken into account in a study aimed at quantifying its properties. Properties spanning tensile strength, fracture toughness, fatigue resistance and resultant fracture behavior can be rationalized for purpose of its selection and use in a desired application. An optical micrograph of the longitudinal section of the as provided stainless steel 2304 is shown in the Figure 5.1. An optical micrograph of the transverse (T) section of the same stainless steel 2304 specimen is shown in Figure 5.2. The longitudinal (L) section reveals a mixture of light and dark regions. The light regions or islands can be categorized as pockets of ferrite (pure iron), while the darker or gray color regions are a mixture of very fine pearlite and austenite.

Also, the longitudinal (L) region revealed an absence of coarse second-phase particles at the allowable magnifications of the light optical microscope. The transverse (T) section of the as-provided material, i.e., stainless steel, reveals a healthy mixture of very fine grains. The light color regions or islands represent ferrite (or pure iron), while the darker regions represent a combination or mixture of pearlite and austenite. The presence and distribution of these micro-constituents is governed by a combination of composition and primary processing technique used to manufacture the as-provided steel. These microstructural features do exert an influence on tensile properties and cyclic fatigue behavior of the candidate steel.

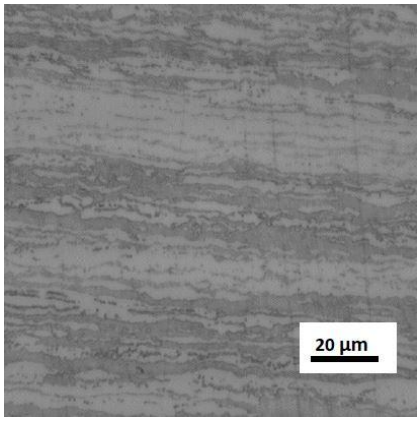

Fig -5.1: Optical micrograph showing key micro-constituents in the longitudinal section of specimen

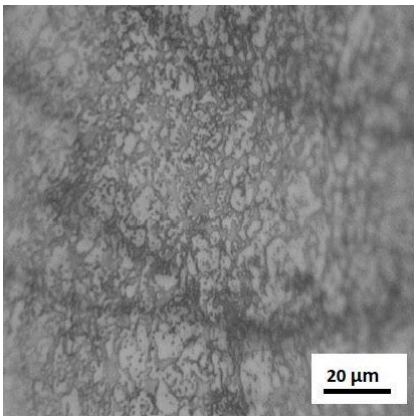

Fig -5.2: Optical micrograph showing key micro-constituents in the transverse section of specimen

5.2 Tensile Properties: Influence of Temperature

Tensile properties of the chosen material (Duplex stainless steel 2304), at both ambient temperature (27^{0}C) and elevated temperature (205 ^{0}C) are summarized in Table 5.3. Results reported are the mean values based on duplicate tests.

(i)The elastic modulus of the chosen steel was 242 GPa at room temperature and 222 Mpa at the elevated temperature of 205 ^{0}C, a nine percent decrease in elastic modulus as a consequence of increase in test temperature.

(ii) Yield strength of the stainless steel at room temperature was 648 MPa and at the elevated temperature 530 Mpa; a noticeable twenty percent decrease in strength with increase in test temperature.

(iii) The ultimate tensile strength (σUTS) at room temperature (27^{0}C) was 808 MPa and 718 Mpa at the elevated temperature (205 ^{0}C), an observable decrease in strength by 11 percent due to increase in test temperature.

(iv)The ductility, quantified by elongation-to-failure was 48.0% at room temperature (27^{0}C) and 40.0% at the elevated temperature (205 ^{0}C).

Table -5.3: A compilation of tensile properties at both room and elevated temperatures (Results are mean values)

Temperature	Elastic Modulus [GPa]	Yield Strength [MPa]	Tensile Strength [MPa]	Ductility [%]
27°C (82 F)	242	648	808	48.0
205°C (400 F)	222	530	718	40.0

5.3 Tensile Fracture Behavior

The tensile fracture surfaces of the chosen material (duplex stainless steel 2304) at both ambient temperature and elevated temperature were examined in a scanning electron microscope (SEM) to provide useful information relating to the specific role of intrinsic microstructural features and microstructural effects on strength, ductility and fracture properties of the candidate steel.

5.3.1 Tensile Fracture at Ambient Temperature

Scanning electron micrographs of the tensile fracture surface of the sample tested at ambient temperature revealed fracture to occur by the characteristic "cup and cone" type of separation, which is an indication of ductile fracture. The overall morphology is shown in Figure 5.3(a). High magnification observation of the fracture surface in the region of early damage initiation revealed in an array of fine microscopic voids and dimples. These features are clearly indicative of locally operating ductile failure mechanisms. This can be seen in Figure 5.3 (b). The fine microscopic cracks were surrounded by an observable population of microscopic voids and dimples, as shown in Figure 5.3(c). These fine features are indicative of "locally" brittle and ductile failure mechanisms. The region of overload revealed a sizeable population of microscopic voids inter-dispersed with shallow dimples (Figure 5.3 (d)), which is indicative of the occurrence of 'locally' ductile failure mechanism.

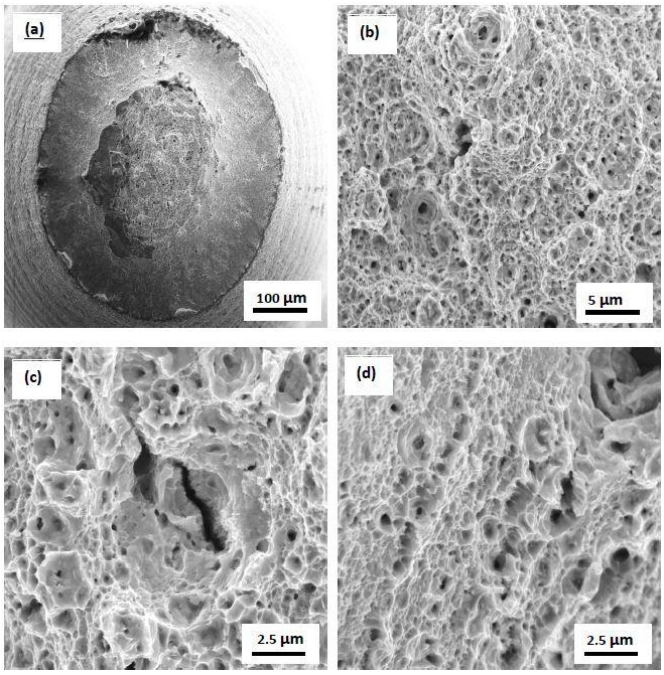

Fig -5.3: Scanning electron micrographs of the tensile fracture surface of stainless steel 2304 deformed at room temperature (27^{0}C), showing:
(a) Overall morphology of failure.
(b) High magnification observation of the region of early damage initiation inlaid with an array of fine microscopic voids and dimples, features indicative of locally ductile failure mechanisms.
(c) Fine microscopic cracks surrounded by an observable population of microscopic voids and dimples indicative of locally brittle and ductile failure mechanisms.
(d) A sizeable population of microscopic voids inter-dispersed with shallow dimples in the region of overload indicative of 'locally' ductile failure mechanism.

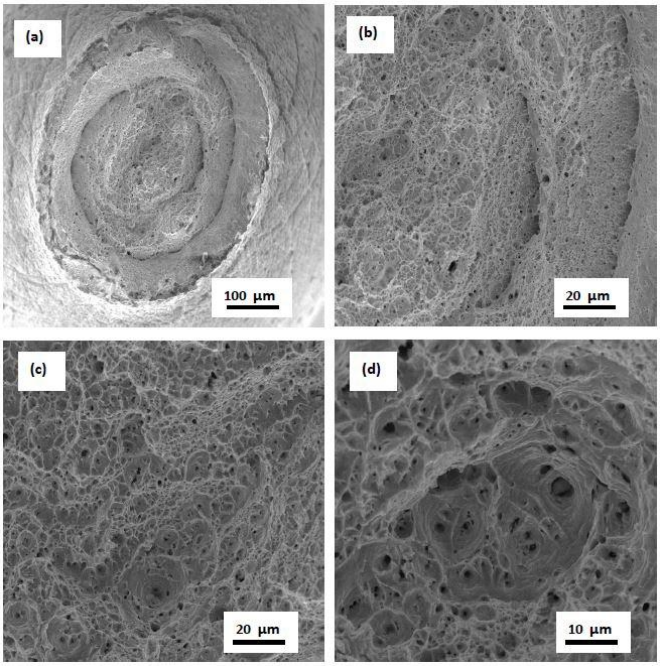

Fig -5.4: Scanning electron micrographs of the sample of stainless steel 2304 deformed in tension at an elevated temperature of 205^{0}C, showing:
(a) Overall morphology of failure revealing cup and cone morphology
(b) High magnification observation of (a) revealing dimples of varying size, isolated microscopic voids and macroscopic crack; features indicative of both brittle and ductile failure mechanism.
(c) A sizeable population of microscopic voids inter-dispersed with dimples, features indicative of 'locally' ductile failure mechanism.
(d) A population of voids of varying size and dimples covering the overload fracture surface.

5.3.2 Tensile Fracture at Elevated Temperature

Scanning electron microscopy observations of the sample of stainless steel 2304 deformed in tension at the chosen elevated temperature [205^{0}C], revealed the following observations. Overall morphology of failure was ductile as shown in Figure 5.4(a). The overall morphology was essentially cup and cone failure. High magnification observation of the fracture surface reveals many features. These features are a combination of dimples of varying size, isolated microscopic voids, and macroscopic cracks (Figure 5.4 (b)). These features are indicative of both brittle and ductile failure mechanisms acting at the fine microscopic level. Figure 5.4(c), a sizeable population of microscopic voids interdispersed with dimples can be seen. These features are indicative of 'locally' ductile failure mechanism. The overload fracture surface revealed a population of voids of varying size and dimples covering the fracture surface (Figure 5.4 (d)). These features are indicative of the occurrence of locally dominant ductile failure mechanisms.

6. CONCLUSIONS

Based on a preliminary study of microstructure and the role of test temperature in influencing tensile properties and fracture behavior of stainless steel 2304, following are the key observations or conclusions:

1. The longitudinal (L) section revealed a mixture of light and dark regions. The light regions or islands can be categorized as pockets of ferrite (pure iron), while the darker or gray color regions are a mixture of very fine pearlite and austenite. Also, the longitudinal (L) region revealed an absence of coarse second-phase particles at the allowable magnifications of the light optical microscope. The transverse (T) section of the as-provided material, i.e., stainless steel, revealed a healthy mixture of very fine grains. The light color regions or islands represent ferrite (or pure iron), while the darker

regions represent a combination or mixture of pearlite and austenite.

2. The presence and distribution of these micro-constituents is governed by a combination of composition and primary processing technique used to manufacture the as-provided steel. These microstructural features do exert an influence on tensile properties and cyclic fatigue behavior of the candidate steel.
3. The elastic modulus of the chosen steel was 242 GPa at room temperature and 222 MPa at the elevated temperature of 400 F, a nine percent decrease in elastic modulus as a consequence of increase in test temperature. Yield strength of the stainless steel at room temperature was 648 MPa and at the elevated temperature 530 Mpa; a noticeable twenty percent decrease in strength with increase in test temperature. The ultimate tensile strength (σUTS) at room temperature (27^0C) was 808 MPa and 718 MPa at the elevated temperature (205^0C), an observable decrease in strength by 11 percent due to increase in test temperature. The ductility, quantified by elongation-to-failure was 48.0% at room temperature (27^0C) and 40.0% at the elevated temperature (205^0C).
4. Tensile fracture at both temperatures was predominantly cup and cone morphology. High magnification observation of the fracture surface revealed a healthy combination of dimples of varying size, isolated microscopic voids, and macroscopic cracks. These features are indicative of both brittle and ductile failure mechanisms acting at the fine microscopic level. At both temperatures, the overload fracture surface revealed a population of voids of varying size and dimples, indicative of the occurrence of "locally" dominant ductile failure mechanisms.

FUTURE SCOPE

Different materials can used to analyze the fracture behavior and compare them. Specimens can be subjected to cyclic fatigue loading and fracture behavior can be analyzed.

REFERENCES

[1] Mechanical Behavior of Materials, N.E. Dowling, Prentice Hall, Upper Saddle River, NJ, 3nd Edition, 2007.
[2] Online material for background of stainless steels http://www.azom.com/article.aspx?ArticleID=470
[3] Online material for the families of stainless steels http://www.azom.com/article.aspx?ArticleID=470#_The_Families_Of
[4] Online material for the charecteristics of stainless steels http://www.azom.com/article.aspx?ArticleID=470#_Characteristics_Of_Stainless
[5] J.F. McGurn, "Stainless Steel Reinforcing Bars in Concrete" Online material http://citeseerx.ist.psu.edu/viewdoc/download?doi=10.1.1.475.5101&rep=rep1&type=pdf
[6] E.S Puchi-Cabrera, F Matinez, Herrera, J.A Berrios, S Dixit, D Bhat: "On the fatigue behavior of an AISI 316L stainless steel coated with a PVD TiN deposit",Surface and Coatings Technology, Volume 182, Issues 2-3, 22 April 2004, Pages 276-286.
[7] K.K. Ray, K. Dutta, S. Sivaprasad, S. Tarafder: " Fatigue damage of AISI 304 LN stainless steel: Role of mean stress", Procedia Engineering, Volume 2,Issue 1, April 2010, Pages 1805-1813.
[8] H Nishi, M Eto, K Tachibana, K Koizumi, M Nakahira, H Takahashi: "Fatigue behavior on weldment of austenitic stainless steel for ITER vacuum vessel", Fusion Engineering and Design, Volumes 58-59, November 2001, Pages 869-873.
[9] M.F. Buchely, H.A. Colorado, H.E. Jaramillo: "Effect of SMAW manufacturing process in high-cycle fatigue of AISI 304 base metal using AISI 308L filler metal",Journal of Manufacturing Processes, Volume 20, Part 1, October 2015, Pages 181-189.
[10] M. Topic, C. Allen, R. Tait: "The effect of cold work and heat treatment on the fatigue behavior of 3CR12 corrosion resistant steel wire", International Journal of Fatigue, Volume 29, Issue 1, January 2007, Pages 49-56.
[11] Zahida Begum, A. Poonguzhali, Ranita Basu, C. Sudha, H. Shaikh, R.V. Subba Rao, Awanikumar Patil, R.K. Dayal: "Studies of the tensile and corrosion fatigue behavior of austenitic stainless steels", Corrosion Science, Volume 53, Issue 4, April 2011, Pages 1424-1432.
[12] Online material for 2304 stainless steel http://stainlessrebar.com
[13] T.S. Srivatsan, K. Manigandan and Thomas Quick: "The Tensile Deformation and Fracture Behavior of Four High Strength Steels," Steel Research International, Vol.82, Issue 12, pp. 1385-1393, 2011
[14] T.S. Srivatsan, K. Manigandan, A. Freborg and T. Quick: "The Quasi Static Deformation and Fracture Behavior of a Novel High Strength Steel for Emerging Applications," Emerging Materials Research, Vol. 2, pp. 17-26, 2013, pp. 17-26.
[15] Patnaik, A., Shan, X., Adams, M., Srivatsan, T. S., Menzemer, C.C., and Payer, J., Isolating Corrosion of Steel Plates Coupled with Titanium, Advanced Steel Construction, Vol. 10, No. 2, June 2014, pp. 216-233.